Korean J. Chem. Eng., **28**(9), 1824-1832 (2011)
DOI: 10.1007/s11814-011-0069-6

Free convective heat and mass transfer in a doubly stratified non-Darcy micropolar fluid

Darbashayanam Srinivasacharya† and Chetteti RamReddy

Department of Mathematics, National Institute of Technology, Warangal-506004, Andhra Pradesh, India
(*Received 5 January 2011 • accepted 16 March 2011*)

Abstract−The flow, heat and mass transfer characteristics of the free convection on a vertical plate with uniform and constant heat and mass fluxes in a doubly stratified micropolar fluid saturated non-Darcy porous medium are studied. The nonlinear governing equations and their associated boundary conditions are initially cast into dimensionless forms by pseudo-similarity variables. The resulting system of equations is then solved numerically using the Keller-box method. The numerical results are compared and found to be in good agreement with previously published results as special cases of the present investigation. The effects of the micropolar, Darcy, non-Darcy and stratification parameters on the dimensionless velocity, microrotation, wall temperature, wall concentration, local skin-friction coefficient and wall couple stress coefficient are presented graphically.

Key words: Free Convection, Non-Darcy Porous Medium, Micropolar Fluid, Double Stratification

INTRODUCTION

Free convection flows in a fluid saturated porous media are of great interest because of their various engineering, scientific and industrial applications in heat transfer. Free convection in porous media occurs in the design of chemical processing equipment, formation and dispersion of fog, distributions of temperature and moisture over agricultural fields and groves of fruit trees and damage of crops due to freezing and pollution of the environment, grain storage systems, heat pipes, packed microsphere insulation, distillation towers, ion exchange columns, subterranean chemical waste migration, solar power absorbers, etc. A number of studies have been reported in the literature focusing on the problem of combined heat and mass transfer in porous media. Nield [1] made the first attempt to study the stability of convective flow in horizontal layers with imposed vertical temperature and concentration gradients. This was followed by Khan and Zebib [2] in the study of flow stability in a vertical porous layer. An analysis of the mass transfer effect on the free convective transport of a viscous fluid past an infinite vertical porous plate was carried out by Soundalgekar [3]. However, Darcy's law is valid only for slow flows through porous media with low permeability. The inertia effect is expected to be important at a higher flow rate and it can be accounted for through the addition of a velocity squared term in the momentum equation, which is known as Forchheimer's extension of Darcy's law. A detailed review of convective heat and mass transfer in Darcian and Non-Darcian porous media, including an exhaustive list of references, can be found in Nield and Bejan [4]. Recently, the absolute and convective instability on mixed convection in porous media was examined by Chung et al. [5].

In many problems of practical interest, natural convection flows arise in a thermally stratified environment. The input of thermal energy in enclosed fluid regions, due to the discharge of hot fluid or heat removal from heated bodies, often leads to the generation of a stable thermal stratification. Stratification of fluid arises due to temperature variations, concentration differences or the presence of different fluids. Several investigations have explored the importance of convective heat and mass transfer in doubly stratified porous media using Darcian and non-Darcian models. Previous studies (for a comprehensive review see Gebhart et al. [6]) have shown that stratification increases the local heat transfer coefficient and decreases the velocity and buoyancy levels. Another considerable effect of the stratification on the mean field is the formation of a region with a temperature deficit (i.e., a negative dimensionless temperature) and flow reversal in the outer part of the boundary layer. This phenomenon was first shown theoretically by Prandtl [7] for an infinite wall and later on by Jaluria and Himasekhar [8] for semi-infinite walls. A combined heat and mass transfer process by natural convection along a vertical wavy surface in a thermal and mass stratified fluid saturated porous enclosure has been numerically studied by Rathish Kumar and Shalini [10]. Recently, Murthy et al. [9], Lakshi Narayana and Murthy [11,12] reported that the temperature and concentration became negative in the boundary layer depending on the relative intensity of the thermal and solutal stratification.

Only a few experimental studies have been carried out on vertical free convection in a stratified environment. Jaluria and Gebhart [13] studied the stability of the flow adjacent to a vertical plate dissipating a uniform heat flux into a stratified medium both theoretically and experimentally. For this case a theoretical similarity solution exists, in which the ambient stratification varies like $x^{1/5}$, where x is the downstream coordinate. Unlike the case of linear stratification, the flow reversal and temperature deficit in this case (Jaluria and Gebhart [13]), where the variation of the ambient temperature is relatively weak, are extremely small. Recently, a mathematical model was presented for the two-dimensional, steady, incompressible, laminar free convection flow boundary layer flow over a continuously moving plate immersed in a thermally-stratified high-porosity non-Darcian porous medium by Anwar Beg et al. [14].

The effects of heat and mass transfer in non-Newtonian fluid have great significance in engineering applications, such as thermal design of industrial equipment dealing with molten plastics, polymeric liq-

†To whom correspondence should be addressed.
E-mail: dsrinivasacharya@yahoo.com, dsc@nitw.ac.in

uids, foodstuffs, or slurries. Yoon et al. [15] studied analytically the linear stability in order to investigate the viscoelastic effects of saturated liquids on the onset conditions in connection with oscillatory instabilities at the threshold of stationary convection. Cheng [16] considered the combined heat and mass transfer on natural convection flow from a vertical wavy surface in a power-law fluid saturated porous medium with thermal and mass stratification. The micropolar fluid model introduced by Eringen [17] exhibits some microscopic effects arising from the local structure and micro-motion of the fluid elements. Further, they can sustain couple stresses. Micropolar fluids have been shown to accurately simulate the flow characteristics of polymeric additives, geomorphological sediments, colloidal suspensions, haematological suspensions, liquid crystals, lubricants, etc. The mathematical theory of equations of micropolar fluids and applications of these fluids in the theory of lubrication and porous media are presented by Lukaszewicz [18]. The heat and mass transfer in micropolar fluids is also important in the context of chemical engineering, aerospace engineering and also industrial manufacturing processes. Micropolar flow and transport in porous media have received less attention despite important applications in emulsion filtration, polymer gel dynamics in packed beds, petroleum and lubrication flows in porous wafers. Ahmadi [19] obtained a self-similar solution of incompressible micropolar boundary layer flow over a semi-infinite flat plate. Free convection boundary-layer flow of a micropolar fluid from a vertical flat plate is examined by Rees and Pop [20]. They solved the governing non-similar boundary-layer equations numerically using the Keller-box method for a range of values of micropolar fluid parameters. Hassanien et al. [21] have considered natural convection flow of micropolar fluid along a vertical and a permeable semi-infinite plate embedded in a porous medium. The problem of fully developed natural convection heat and mass transfer of a micropolar fluid between porous vertical plates with asymmetric wall temperatures and concentrations is analyzed by Abdulaziz and Hashim [22]. The two-dimensional steady-state boundary layer flow of an incompressible micropolar fluid in a Darcian porous medium is studied theoretically and computationally by Zueco et al. [23]. Awad and Sibanda [24] have presented the problem of free convection of heat and mass in micropolar fluid in a channel subject to cross diffusion (namely the Soret and Dufour effects). Rahman et al. [25] analyzed the heat transfer process in a two-dimensional steady hydromagnetic natural convective flow of a micropolar fluid over an inclined permeable plate subjected to a constant heat flux condition. Anuar [26] presented the effects of radiation on the thermal boundary layer flow induced by a linearly stretching sheet immersed in an incompressible micropolar fluid with constant surface temperature. The unsteady laminar flow of an incompressible micropolar fluid over a stretching sheet with prescribed surface heat flux is investigated by Bachok et al. [27]. More recently, Srinivasacharya and RamReddy [28] studied the mixed convection heat and mass transfer along a vertical plate embedded in a micropolar fluid saturated non-Darcy porous medium by taking into account the linear thermal and solutal stratification effects.

The natural convection on a vertical plate with constant and uniform heat and mass fluxes in a micropolar fluid in the presence of linear stratification with non-Darcy effects has not been reported in the literature. This type of investigation is useful in understanding heat and mass transfer characteristics around a hot radioactive subsurface storage site or around a cooling magmatic intrusion where the theory of convection heat and mass transport is involved. Hence, these boundary conditions are physically realistic and have more practical relevance. This work aims to study a mathematical model for the steady free convection heat and mass transfer in a micropolar fluid in the presence of significant thermal and mass stratification, non-Darcian effects on a vertical plate with uniform heat and mass fluxes. Keller-box method [29] is employed to solve the nonlinear system of governing equations of this particular problem. The effects of micropolar, Darcy, non-Darcy, thermal and solutal stratification parameters on the velocity, microrotation, temperature and concentration are examined. The results are compared with relevant results in the existing literature and are found to be in good agreement.

MATHEMATICAL FORMULATION

Consider the free convection heat and mass transfer along a vertical plate of length L embedded in a stable, doubly stratified micropolar fluid saturated non-Darcy porous medium. The porous medium is considered to be homogeneous and isotropic (i.e., uniform with a constant porosity and permeability), and is saturated with a fluid which is in local thermodynamic equilibrium with the solid matrix. The fluid has constant properties except the density in the buoyancy term of the balance of momentum equation. The fluid flow is moderate, so the pressure drop is proportional to the linear combination of fluid velocity and the square of velocity (Forchheimer flow model is considered). Also, the fluid flow is steady, laminar and two dimensional. We choose the coordinate system such that x-axis is along the vertical plate and y-axis is normal to the plate. The physical model and coordinate system are shown in Fig. 1. The plate is maintained at uniform and constant heat and mass fluxes q_w and q_m respectively. The temperature and the mass concentration of the ambient medium are assumed to be linearly stratified in the form $T_\infty(x)=T_{\infty,0}+Ax$ and $C_\infty(x)=C_{\infty,0}+Bx$, respectively, where A and B are constants and varied to alter the intensity of stratification in the medium and $T_{\infty,0}$ and $C_{\infty,0}$ are ambient temperature and concentration, respectively.

By employing laminar boundary layer flow assumptions, Boussinesq approximation, using the Darcy-Forchheimer model and Dupuit-Forchheimer relationship [4], the governing equations for the micropolar fluid are given by

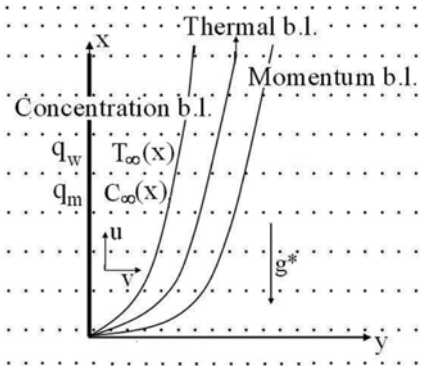

Fig. 1. Physical model and coordinate system.

$$\frac{\partial u}{\partial x}+\frac{\partial v}{\partial y}=0 \tag{1}$$

$$\frac{\rho}{\varepsilon^2}\left(u\frac{\partial u}{\partial x}+v\frac{\partial u}{\partial y}\right)=\frac{(\mu+\kappa)}{\varepsilon}\frac{\partial^2 u}{\partial y^2}+\kappa\frac{\partial \omega}{\partial y}+\rho g^*(\beta_T(T-T_\infty)+\beta_C(C-C_\infty))-\frac{\mu}{K_p}u-\frac{\rho b}{K_p}u^2 \tag{2}$$

$$\frac{\rho j}{\varepsilon}\left(u\frac{\partial \omega}{\partial x}+v\frac{\partial \omega}{\partial y}\right)=\gamma\frac{\partial^2 \omega}{\partial y^2}-\kappa\left(2\omega+\frac{1}{\varepsilon}\frac{\partial u}{\partial y}\right) \tag{3}$$

$$u\frac{\partial T}{\partial x}+v\frac{\partial T}{\partial y}=\alpha\frac{\partial^2 T}{\partial y^2} \tag{4}$$

$$u\frac{\partial C}{\partial x}+v\frac{\partial C}{\partial y}=D\frac{\partial^2 C}{\partial y^2} \tag{5}$$

where u and v are the Darcy velocity components in x and y directions, respectively, ω is the component of micro-rotation whose direction of rotation lies in the xy-plane, T is the temperature, C is the concentration, g* is the acceleration due to gravity, ρ is the density, μ is the dynamic coefficient of viscosity, b is the Forchheimer constant, K_p is the permeability, ε is the porosity, β_T is the coefficient of thermal expansion, β_C is the coefficient of solutal expansions, κ is the vortex viscosity, j is the micro-inertia density, γ is the spin-gradient viscosity, α and D are the effective thermal and solutal diffusivities of the medium. The last two terms on the right hand side of Eq. (2) stand for the first-order (Darcy) resistance and second-order porous inertia resistance, respectively. The microrotation represents the rotation in an average sense of the rigid particles centered in a small volume element about the centroid of the element.

The boundary conditions are

$$u=0,\ v=0,\ \omega=0,\ q_W=-k\left.\frac{\partial T}{\partial y}\right|_{y=0},\ q_m=-D\left.\frac{\partial C}{\partial y}\right|_{y=0}$$

at y=0 (6a)

u=0, ω=0, T=T_∞(x), C=C_∞(x) as y$\to\infty$ (6b)

where k is the thermal conductivity of the fluid and the boundary condition ω=0 in Eq. (6a), represents the case of concentrated particle flows in which the microelements close to the wall are not able to rotate [30].

In view of the continuity Eq. (1), we introduce the stream function ψ by

$$u=\frac{\partial \psi}{\partial y},\ v=-\frac{\partial \psi}{\partial x} \tag{7}$$

Substituting Eq. (7) in Eqs. (2)-(5) and then using the following pseudo-similarity transformations

$$\left.\begin{aligned}\xi&=\frac{x}{L},\ \eta=\frac{Gr^{1/5}}{L\xi^{1/5}}y,\\ \psi&=\frac{\mu Gr^{1/5}\xi^{4/5}}{\rho}f(\xi,\eta),\\ \omega&=\frac{\mu Gr^{3/5}\xi^{2/5}}{\rho L^2}g(\xi,\eta),\\ T-T_\infty(x)&=\frac{q_w L}{k}\xi^{1/5}Gr^{-1/5}\theta(\xi,\eta),\\ C-C_\infty(x)&=\frac{q_m L}{D}\xi^{1/5}Gr^{-1/5}\phi(\xi,\eta)\end{aligned}\right\} \tag{8}$$

we get the following nonlinear system of differential equations

$$\left(\frac{1}{\varepsilon(1-N)}\right)f'''+\frac{4}{5\varepsilon^2}f\ f''-\frac{3}{5\varepsilon^2}(f')^2+\left(\frac{N}{1-N}\right)g'+\theta+\mathcal{B}\phi-\frac{1}{DaGr^{2/5}}\xi^{2/5}f'-\frac{Fs}{Da}\xi f'^2=\frac{\xi}{\varepsilon^2}\left(f'\frac{\partial f'}{\partial \xi}-f''\frac{\partial f}{\partial \xi}\right) \tag{9}$$

$$\lambda g''+\frac{4}{5\varepsilon}fg'-\frac{2}{5\varepsilon}f'g-\left(\frac{N}{1-N}\right)\mathcal{G}\xi^{2/5}\left(2g+\frac{1}{\varepsilon}f''\right)=\frac{\xi}{\varepsilon}\left(f'\frac{\partial g}{\partial \xi}-g'\frac{\partial f}{\partial \xi}\right) \tag{10}$$

$$\frac{1}{Pr}\theta''+\frac{4}{5}f\theta'-\frac{1}{5}f'\theta-\varepsilon_1\xi^{4/5}f'=\xi\left(f'\frac{\partial \theta}{\partial \xi}-\theta'\frac{\partial f}{\partial \xi}\right) \tag{11}$$

$$\frac{1}{Sc}\phi''+\frac{4}{5}f\phi'-\frac{1}{5}f'\phi-\varepsilon_2\xi^{4/5}f'=\xi\left(f'\frac{\partial \phi}{\partial \xi}-\phi'\frac{\partial f}{\partial \xi}\right) \tag{12}$$

where the primes indicate partial differentiation with respect to η alone, Gr=($g^*\beta_T q_w L^4$)/kν^2 is the thermal Grashof number, Pr=ν/α is the Prandtl number, Sc=ν/D is the Schmidt number, Da=K_p/L^2 is the Darcy number, Fs=b/L is the Forchheimer number, N=$\kappa/(\kappa+\mu)$ ($0\le N<1$) is the Coupling number [30], $\mathcal{G}=L^2/jGr^{2/5}$ is the micro-inertia density, $\lambda=\gamma/j\rho\nu$ is the spin-gradient viscosity and $\mathcal{B}$=k$\beta_C q_m$/D$\beta_T q_w$ is the buoyancy ratio. When, $\mathcal{B}$=0 the flow is driven by thermal buoyancy alone. $\varepsilon_1=(k/q_w)Gr^{1/5}(\partial T_\infty/\partial x)$ and $\varepsilon_2=(D/q_m)Gr^{1/5}(\partial C_\infty/\partial x)$ are the thermal and solutal stratification parameters, respectively.

The boundary conditions (6) in terms of f, g, θ and ϕ become

$$\eta=0\text{: } f'(\xi,0)=0,\ f(\xi,0)=-\frac{5}{4}\xi\left(\frac{\partial f}{\partial \xi}\right)_{\eta=0},$$

$$g(\xi,0)=0,\ \theta'(\xi,0)=-1,\ \phi'(\xi,0)=-1 \tag{13a}$$

$$\eta\to\infty\text{: } f'(\xi,\infty)=0,\ g(\xi,\infty)=0,\ \theta(\xi,\infty)=0,\ \phi(\xi,\infty)=0 \tag{13b}$$

If Da$\to\infty$, ε=1, ε_1=0 and ε_2=0, the problem reduces to free convection on a vertical plate with uniform and constant heat and mass fluxes in unstratified micropolar fluid. In the limit, as N$\to$0, the governing Eqs. (1)-(5) reduce to the corresponding equations for a viscous fluid. Hence, the case of the mixed convection heat transfer in an unstratified Newtonian fluid flow along a cylinder of Lee et al. [32] can be obtained by taking N=0, $\mathcal{B}$=0, ε=1, Da$\to\infty$, ε_1=0 and ε_2=0, who investigated the mixed convection heat transfer in an unstratified Newtonian fluid flow along a cylinder.

The wall shear stress and the wall couple stress are

$$\tau_w=\left[(\mu+\kappa)\frac{\partial u}{\partial y}+\kappa\omega\right]_{y=0},\ m_w=\gamma\left[\frac{\partial \omega}{\partial y}\right]_{y=0} \tag{14}$$

and the heat and mass transfers from the plate respectively are given by

$$q_w=-k\left(\frac{\partial T}{\partial y}\right)_{y=0},\ q_m=-D\left(\frac{\partial C}{\partial y}\right)_{y=0} \tag{15}$$

The dimensionless skin friction $C_f=2\tau_w/\rho U_*^2$, wall couple stress $M_w=m_w/\rho U_*^2 L$, the local Nusselt number $Nu_x=q_w x/(k(T_w-T_{\infty,0}))$ and local Sherwood number $Sh_x=q_m x/(D(C_w-C_{\infty,0}))$ where U_* is the characteristic velocity, are given by

$$C_f=\left(\frac{2}{1-N}\right)Gr_x^{-1/5}f''(\xi,0), \tag{16a}$$

$$M_w=\left(\frac{\lambda}{\mathcal{G}}\right)\xi^{3/5}Gr_x^{-2/5}g'(\xi,0) \tag{16b}$$

$$\frac{Nu_x}{Gr_x^{1/5}} = \frac{1}{\theta(\xi,0) + \varepsilon_1 \xi^{4/5}}, \tag{16c}$$

$$\frac{Sh_x}{Gr_x^{1/5}} = \frac{1}{\phi(\xi,0) + \varepsilon_2 \xi^{4/5}} \tag{16d}$$

where $Gr_x=(g^*\beta_1 q_w x^4)/k\nu^2$ is the local thermal Grashof number.

RESULTS AND DISCUSSIONS

The flow Eqs. (9) and (10) which are coupled, together with the energy and concentration Eqs. (11) and (12), constitute non-linear non-homogeneous differential equations for which closed-form solutions cannot be obtained and hence we have to solve the problem numerically. Hence the governing boundary layer Eqs. (9) to (12) have been solved numerically using the Keller-box implicit method [29]. This method, which is adequately explained in the literature, also gives accurate results for boundary layer equations. In the present study the boundary conditions for η at ∞ are replaced by a sufficiently large value of η where the velocity, microrotation, temperature and concentration profiles approach 0. We have taken η_∞=15 and a grid size of η of 0.01. We have computed the solutions for the non-dimensional velocity, angular momentum, temperature and concentration profiles as shown graphically in Figs. 2-6. The effect of micropolar parameter N, non-Darcy parameter Fs, Darcy number Da and stratification parameters, ε_1 and ε_2 has been discussed. To reduce the number of parameters involved, computations were carried out for the cases of ε=0.6, ξ=0.1, Gr=5, $\mathcal{B}$=1, Pr=0.71 and Sc=0.22 while N, Fs, Da, ε_1 and ε_2 were varied over a range. The values $\mathcal{G}$=5, λ=5 are chosen so as to satisfy the thermodynamic restrictions on the material parameters given by Eringen [17].

In the absence of coupling number N, stratification parameters ε_1 and ε_2 with $\mathcal{G}$=0, λ=0, Da$\to\infty$, ε=1 and $\mathcal{B}$=0, the results have been compared with that of previous work [32], and it is found that they are in good agreement, as shown in Table 1. Therefore, the developed code can be used with great confidence to study the problem considered in this paper.

The coupling number N characterizes the coupling of linear and rotational motion arising from the micromotion of the fluid mole-

Table 1. Comparison of results for a vertical plate with unstratified case [32]

$\frac{Nu_x}{Gr_x^{1/5}} = \frac{1}{\theta(\xi,0)}$		
Pr	Lee et al. [32]	Present
0.1	0.2634	0.2634
0.7	0.4838	0.4838
7.0	0.8697	0.8692
10	1.5546	1.5540

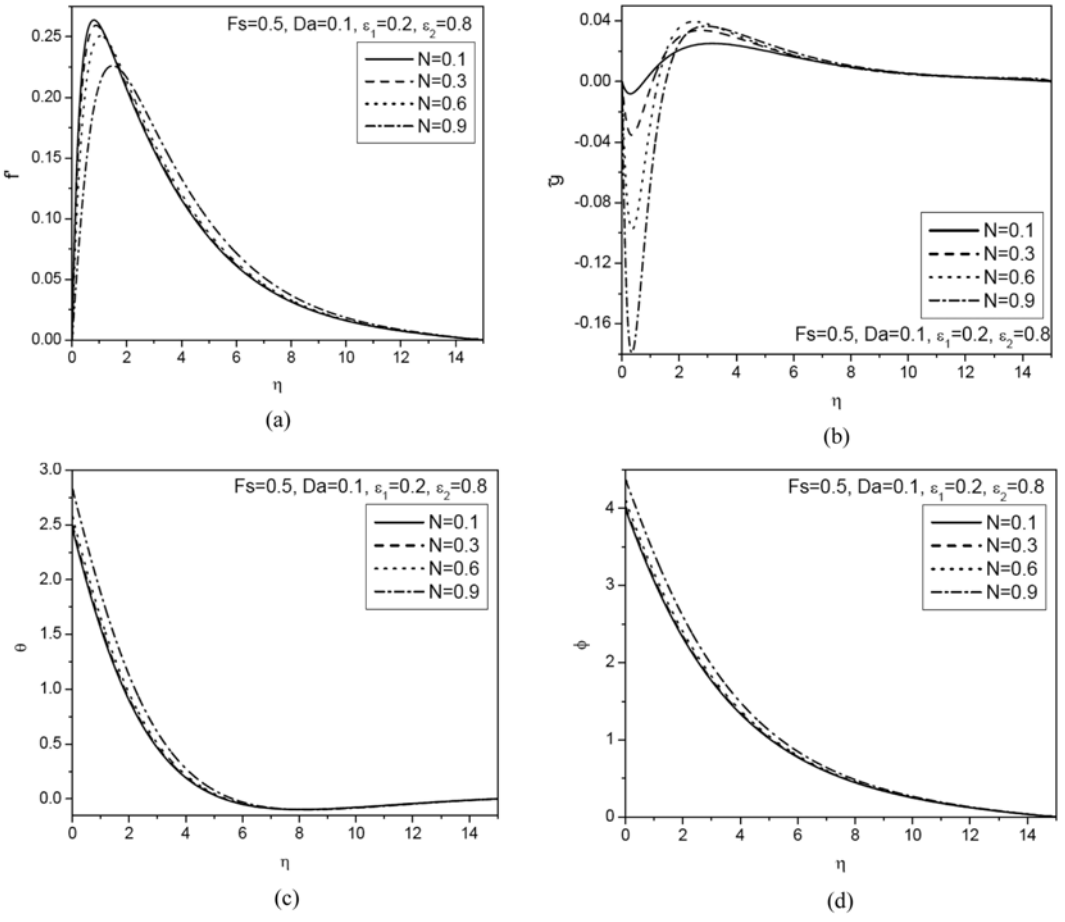

Fig. 2. (a) Velocity, (b) Microrotation, (c) Temperature and (d) Concentration profiles for various values of N.

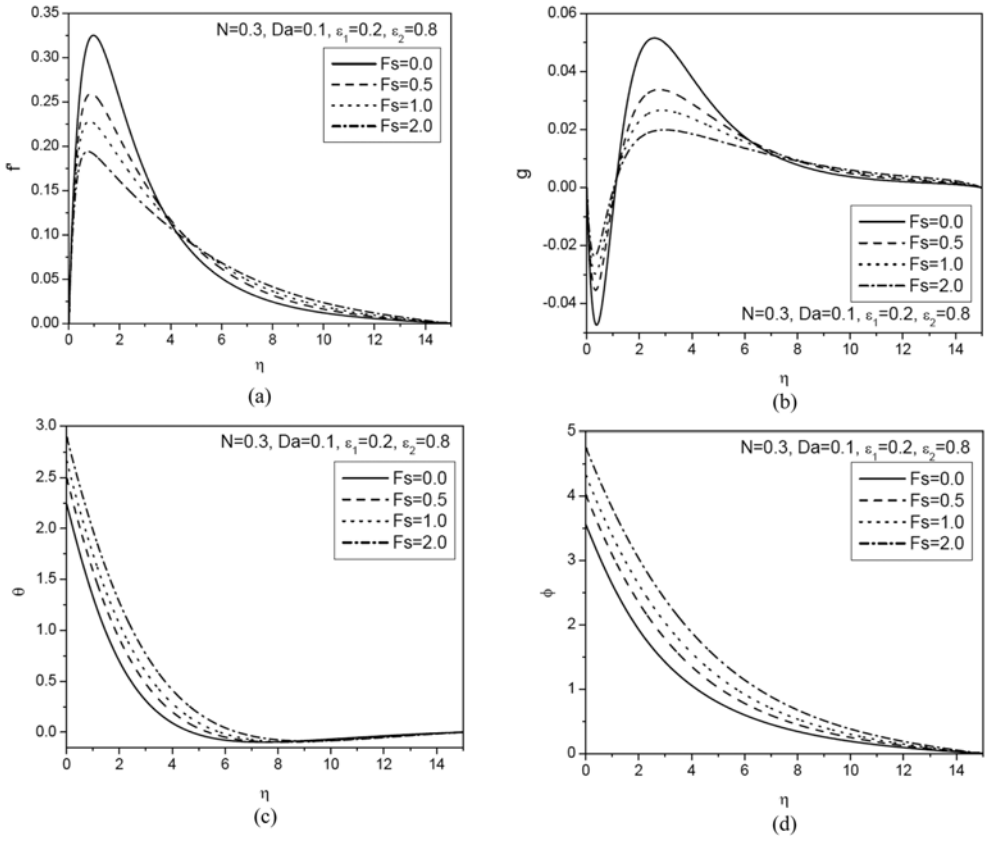

Fig. 3. (a) Velocity, (b) Microrotation, (c) Temperature and (d) Concentration profiles for various values of Fs.

cules. Hence N signifies the coupling between the Newtonian and rotational viscosities. With a large value of N the effect of microstructure becomes significant, whereas with a small value of N the individuality of the substructure is much less pronounced. As κ tends to zero, N also tends to zero, the micro-polarity is lost and the fluid behaves as a non-polar fluid.

In Figs. 2(a)-2(d), the effect of the coupling number N on the dimensionless velocity, microrotation, temperature and concentration profiles is presented for fixed values of Fs, Da, ε_1 and ε_2. As N increases, it can be observed from Fig. 2(a) that the velocity maximum decreases in amplitude and the location of the maximum velocity moves farther away from the wall. The velocity in case of micropolar fluid is less than that of the viscous fluid (N→0 corresponds to viscous fluid). From Fig. 2(b), we observe that the microrotation changes sign from negative to positive within the boundary layer. The microrotation tends to zero as N→0 as is expected that in the limit $\kappa \to 0$ i.e., N→0, the Eqs. (1) and (2) are uncoupled with Eq. (3) and they reduce to viscous fluid flow equations. It is clear from Fig. 2(c) that the temperature increases with the increase of coupling number N. It can be seen from Fig. 2(d) that the concentration of the fluid increases with the increase of coupling number N. The temperature and concentration in case of micropolar fluids is more than that of the corresponding Newtonian fluid case.

The dimensionless velocity distribution for different values of Forchheimer number Fs for fixed values of N, Da, ε_1 and ε_2, is depicted in Fig. 3(a). Since Fs represents the inertial drag, thus an increase in the Forchheimer number increases the resistance to the flow and so a decrease in the fluid velocity ensues. Here Fs=0 represents the case where the flow is Darcian. The velocity is maximum in this case due to the total absence of inertial drag. From Fig. 3(b), the microrotation changes in sign from negative to positive values at the critical point η=1.05 within the boundary layer. The dimensionless temperature for different values of Forchheimer number for N, Da, ε_1 and ε_2, is displayed in Fig. 3(c). An increase in Forchheimer number, Fs, increases temperature values, since as the fluid is decelerated, energy is dissipated as heat and serves to increase temperature. As such the temperature is minimized for the lowest value of Fs and maximized for the highest value of Fs as shown in Fig. 3(c). Fig. 3(d) demonstrates the dimensionless concentration for different values of Forchheimer number with N, Da, ε_1 and ε_2. As the Forchheimer number increases, the concentration boundary layer thickness increases. The increase in non-Darcy parameter reduces the intensity of the flow but enhances the thermal and concentration boundary layer thicknesses.

Figs. 4(a)-4(d) illustrate the influence of Darcy number Da, on the velocity, micro-rotation, temperature and concentration profiles. Fig. 4(a) indicates that a rise in Da (which implies a rise in permeability, K_p) enhances considerably the velocity of the micropolar fluid near the wall and its behavior reverses far away from the wall. With increasing permeability the porous matrix structure becomes less and less prominent and in the limit of infinite Da values (i.e., $(1/\mathrm{Da}\,\mathrm{Gr}^{2/5}) \to 0$ and $(\mathrm{Fs}/\mathrm{Da})f'^2 \to 0$), the porosity vanishes and the present problem reduces to a purely free convective heat and mass transfer in a micropolar fluid with thermal and solutal stratification. Forchheimer drag is clearly inversely proportional to Da (and velocity gradient) for constant Fs. From Fig. 4(b), we notice that the microro-

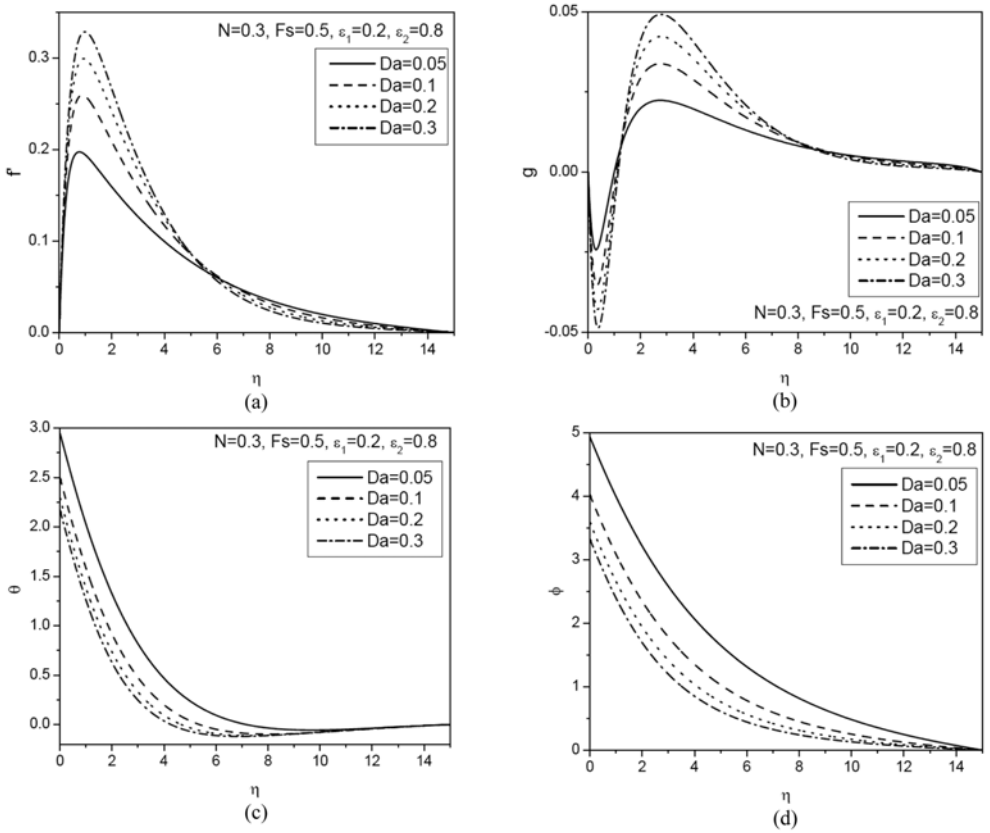

Fig. 4. (a) Velocity, (b) Microrotation, (c) Temperature and (d) Concentration profiles for various values of Da.

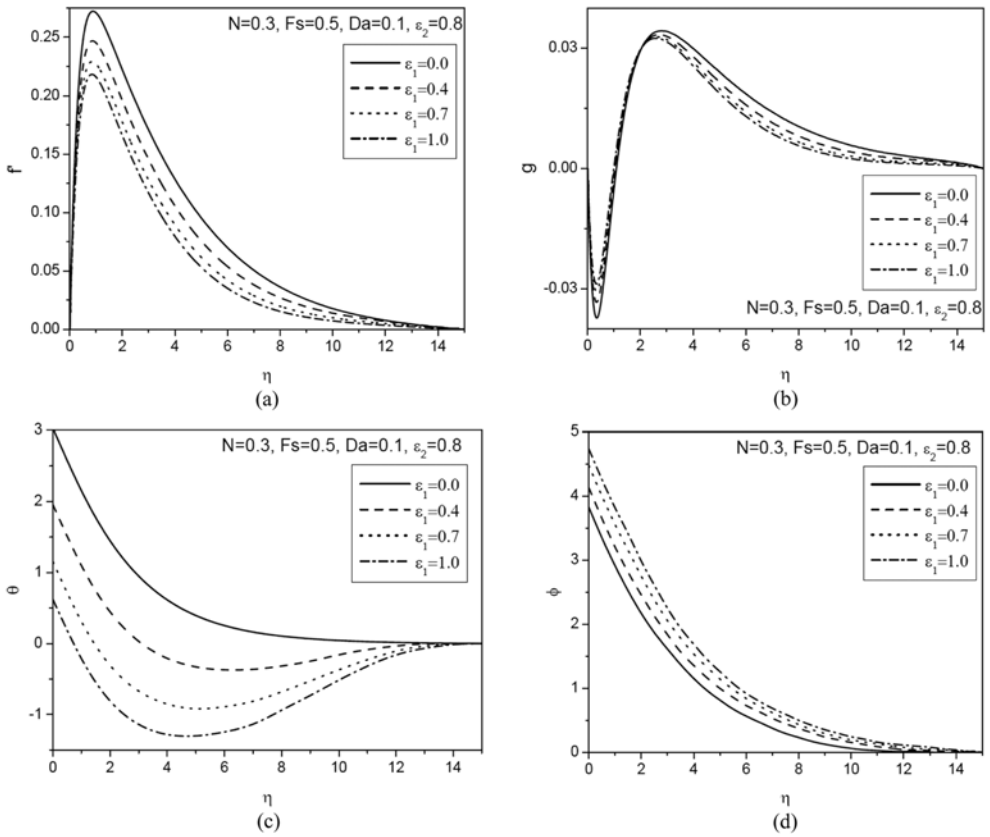

Fig. 5. (a) Velocity, (b) Microrotation, (c) Temperature and (d) Concentration profiles for various values of ε_1.

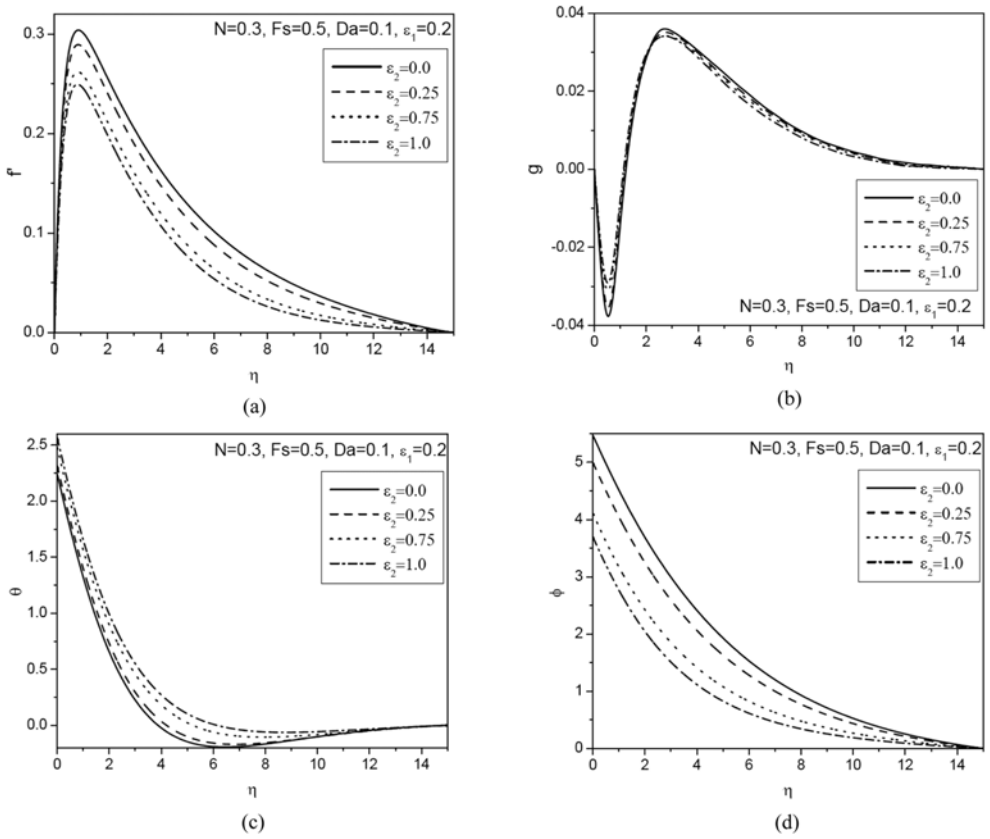

Fig. 6. (a) Velocity, (b) Microrotation, (c) Temperature and (d) Concentration profiles for various values of ε_2.

tation changes sign from negative to positive values at the critical point η=1.05 within the boundary layer. The dimensionless temperature for different values of Darcy number for N=0.3, Fs=0.5, ε_1=0.2 and ε_2=0.8, is depicted in Fig. 4(c). The temperature of the fluid decreases with the increase of Darcy number. Fig. 4(d) illustrates that non-dimensional concentration for various values of the Darcy number for N=0.3, Fs=0.5, ε_1=0.2 and ε_2=0.8. The figure shows that concentration decreases with the increase in the Darcy number.

Fig. 5(a) displays the non-dimensional velocity for different values of thermal stratification parameter ε_1 for fixed values of N, Fs, Da and ε_2. Also, it can be noted that the velocity of the fluid decreases with the increase of thermal stratification parameter. This is because thermal stratification reduces the effective convective potential between the heated plate and the ambient fluid in the medium. Hence, the thermal stratification effect reduces the velocity in the boundary layer. From Fig. 5(b), we observe that the microrotation changes sign from negative to positive values at the critical point η=1.05 within the boundary layer. The dimensionless temperature for different values of thermal stratification parameter for N=0.3, Fs=0.5, Da=0.1 and ε_2=0.8, is shown in Fig. 5(c). It is evident that the temperature of the fluid decreases with the increase of thermal stratification parameter. When the thermal stratification effect is taken into consideration, the effective temperature difference between the plate and the ambient fluid will decrease; therefore, the thermal boundary layer is thickened and the temperature is reduced. Fig. 5(d) shows the dimensionless concentration for different values of thermal stratification parameter for N=0.3, Fs=0.5, Da=0.1 and ε_2=0.8. The concentration of the fluid increases with the increase of thermal stratification parameter. It can be noted that the effect of the stratification on the temperature is the formation of a region with a temperature deficit (i.e., a negative dimensionless temperature). This is in tune with the observation made in Refs [Gebhart et al. [6]; Prandtl [7]; Jaluria and Himasekhar [8]; Murthy et al. [9]; Lakshmi Narayana and Murthy [11,12]].

The dimensionless velocity component for different values of solutal stratification parameter, ε_2, with constant coupling number, N, Forchheimer number, Fs, Darcy number, Da, and thermal stratification parameter, ε_1, is depicted in Fig. 6(a). The velocity of the fluid decreases with the increase of solutal stratification parameter. From Fig. 6(b), we observe that the microrotation changes sign from negative to positive values at the critical point η=1.05 within the boundary layer. The dimensionless temperature for different values of solutal stratification parameter for N=0.3, Fs=0.5, Da=0.1 and ε_1=0.2, is displayed in Fig. 6(c). The temperature of the fluid increases with the increase of solutal stratification parameter. Fig. 6(d) demonstrates the dimensionless concentration for different values of solutal stratification parameter with N=0.3, Fs=0.5, Da=0.1 and ε_1=0.2. It is clear that the concentration of the fluid decreases with the increase of thermal stratification parameter. Hence, compared with the unstratified fluid (i.e., ε_1=ε_2=0), an increase in the stratification parameters, ε_1 and ε_2, causes a reduction in the velocity boundary layer thickness.

Table 2 shows the effect of the coupling number N, on the skin friction coefficient $f''(\xi, 0)$ and the dimensionless wall couple stress $g'(\xi, 0)$. The skin friction coefficient is lower for micropolar fluid

Table 2. Effect of skin friction and wall couple stress for various values of N, Fs, Da, ε_1 and ε_2

N	Fs	Da	ε_1	ε_2	$f''(\xi, 0)$	$-g'(\xi, 0)$
0.0	0.5	0.1	0.2	0.8	1.14291	0.00000
0.1	0.5	0.1	0.2	0.8	1.08373	0.06738
0.3	0.5	0.1	0.2	0.8	0.95110	0.25555
0.6	0.5	0.1	0.2	0.8	0.69685	0.67551
0.9	0.5	0.1	0.2	0.8	0.30088	1.39629
0.3	0.0	0.1	0.2	0.8	0.99079	0.30494
0.3	0.5	0.1	0.2	0.8	0.95110	0.25555
0.3	1.0	0.1	0.2	0.8	0.92971	0.23024
0.3	1.5	0.1	0.2	0.8	0.91463	0.21339
0.3	2.0	0.1	0.2	0.8	0.90287	0.20088
0.3	0.5	0.05	0.2	0.8	0.89457	0.20175
0.3	0.5	0.1	0.2	0.8	0.95110	0.25555
0.3	0.5	0.15	0.2	0.8	0.98180	0.28835
0.3	0.5	0.2	0.2	0.8	1.00269	0.31179
0.3	0.5	0.4	0.2	0.8	1.05077	0.36729
0.3	0.5	0.1	0.0	0.8	0.99880	0.26915
0.3	0.5	0.1	0.3	0.8	0.92814	0.24893
0.3	0.5	0.1	0.5	0.8	0.88414	0.23610
0.3	0.5	0.1	0.7	0.8	0.84282	0.22389
0.3	0.5	0.1	1.0	0.8	0.80421	0.21235
0.3	0.5	0.1	0.2	0.00	1.11660	0.30263
0.3	0.5	0.1	0.2	0.25	1.06165	0.28721
0.3	0.5	0.1	0.2	0.50	1.00955	0.27240
0.3	0.5	0.1	0.2	0.75	0.96052	0.25828
0.3	0.5	0.1	0.2	1.00	0.91468	0.24494

than the Newtonian fluids (N=0). This is because micropolar fluids offer a great resistance (resulting from vortex viscosity) to the fluid motion and cause larger skin friction factor compared to Newtonian fluid. The results also indicate that the large values of coupling number N, lower wall couple stresses. The effect of the Forchheimer number Fs, on the skin friction coefficient $f''(\xi, 0)$ and the dimensionless wall couple stress $g'(\xi, 0)$, is represented in Table 2. The skin friction coefficient decreases while the wall couple stress increases as Fs increases. In Table 2, the effect of the Darcy number Da, on the skin friction coefficient $f''(\xi, 0)$ and the dimensionless wall couple stress $g'(\xi, 0)$, is displayed. The skin friction coefficient increases and the wall couple stress decreases as Da increases. The effect of the thermal stratification parameter ε_1, on the skin friction coefficient $f''(\xi, 0)$ and the dimensionless wall couple stress $g'(\xi, 0)$, is presented in Table 2. The skin friction coefficient decreases, whereas the wall couple stress increases as ε_1 increases. The results of Table 2 describe the effect of solutal stratification parameter ε_2, on the skin friction coefficient $f''(\xi, 0)$ and the dimensionless wall couple stress $g'(\xi, 0)$. It is clear that the skin friction coefficient decreases, but the wall couple stress increases as ε_2 increases. Furthermore, the skin friction coefficient is higher and wall couple stress parameter is lower for the unstratified fluid (i.e., $\varepsilon_1=\varepsilon_2=0$) than for the stratified fluid (i.e., $\varepsilon_1>0$ and $\varepsilon_2\neq0$).

CONCLUSIONS

We have presented a boundary layer analysis for free convection flow in a doubly stratified micropolar fluid saturated non-Darcy porous medium over a vertical plate with uniform and constant heat and mass flux conditions. Using the pseudo-similarity variables the governing equations are transformed into a set of non-similar parabolic equations where numerical solution has been presented for a wide range of parameters. The higher values of the coupling number N, result in lower velocity distribution but higher wall temperature, wall concentration distributions in the boundary layer than the Newtonian fluid. An increase in the Forchheimer number Fs, reduces the velocity and the skin friction coefficient, whereas it increases the temperature, concentration distributions and the wall couple stress in the boundary layer. In the case of Darcy number, Da, velocity and skin friction coefficient increase and the temperature, concentration and the wall couple stresses decrease with the increasing values of Da. An increase in the thermal stratification parameter, ε_1, reduces the velocity, temperature distributions and the skin friction coefficient, but increases the concentration distribution and the wall couple stress in the boundary layer. An increase in the solutal stratification parameter, ε_2, reduces the velocity, concentration distributions and the skin friction coefficient, but increases the temperature distribution and the wall couple stress in the boundary layer. We observed that the microrotation changes sign from negative to positive values within the boundary layer. The results indicate that the skin friction and wall couple stresses are reduced in the case of micropolar fluid when compared with the case of Newtonian fluid.

ACKNOWLEDGEMENTS

The authors are thankful to the reviewers for their valuable suggestions and comments.

NOMENCLATURE

A : slope of ambient temperature
b : forchheimer constant
B : slope of ambient concentration
$\mathcal{B}$: buoyancy ratio
C : concentration
C_f : skin friction coefficient
C_w : wall concentration
$C_{\infty,0}$: ambient concentration
D : solutal diffusivity
Da : darcy number
f : reduced stream function
Fs : forchheimer number
g^* : gravitational acceleration
g : dimensionless microrotation
Gr : thermal Grashof number
j : micro-inertia density
$\mathcal{G}$: dimensionless micro-inertia density
k : thermal conductivity
K_p : permeability of porous medium
L : characteristic length of the plate
M_w : dimensionless wall couple stress
m_w : wall couple stress
Nu_x : local Nusselt number
N : coupling number

Pr : prandtl number
q_w, q_m : heat, mass transfers from the plate
Sc : schmidt number
T : temperature
T_w : wall temperature
$T_{\infty,0}$: ambient temperature
U_* : characteristic velocity
u, v : darcy velocity components in x and y directions
x, y : coordinates along and normal to the plate
α : thermal diffusivity
β_T, β_C : coefficients of thermal and solutal expansion
γ : spin-gradient viscosity
η : pseudo-similarity variable
θ : dimensionless temperature
ϕ : dimensionless concentration
κ : vortex viscosity
λ : dimensionless spin-gradient viscosity
μ : dynamic viscosity
ν : kinematic viscosity
ξ : dimensionless streamwise coordinate
ρ : density of the fluid
τ_w : wall shear stress
ψ : stream function
ω : component of microrotation
ε : porosity
ε_1, ε_2 : thermal and solutal stratification parameters

Subscripts

w : wall condition
∞ : ambient condition
C : concentration
T : temperature

Superscript

$'$: differentiation with respect to η.

REFERENCES

1. D. A. Nield, *Water Res.*, **4**, 553 (1968).
2. A. A. Khan and A. Zebib, *J. Heat Transfer*, **103**, 179 (1981).
3. V. M. Soundalgekar, Proceedings of Indian Academy of Science, **84A**, 194 (1976).
4. D. A. Nield and A. Bejan, *Convection in porous media*, 3rd Ed., Springer-Verlag, New York (2006).
5. T. J. Chung, M. C. Kim and C. K. Choi, *Korean J. Chem. Eng.*, **26**, 332 (2009).
6. B. Gebhart, Y. Jaluria, R. Mahajan and B. Sammakia, *Buoyancy lnduced flows and transport*, Hemisphere Publishing Co. (1988).
7. L. Prandtl, *Essentials of fluid dynamics*, Blackie, London (1952).
8. Y. Jaluria and K. Himasekhar, *Comput. Fluids*, **11**, 39 (1983).
9. P. V. S. N. Murthy, D. Srinivasacharya and P. V. S. S. S. R. Krishna, *Trans. ASME J.Heat Transfer*, **126**, 476 (2004).
10. B. V. Rathish Kumar and Shalini, *Appl. Math. Comput.*, **171**, 180 (2005).
11. P. A. Lakshmi Narayana and P. V. S. N. Murthy, *Trans. ASME, J. Heat Transfer*, **128**, 1204 (2006).
12. P. A. Lakshmi Narayana and P. V. S. N. Murthy, *J. Porous Media*, **10**, 613 (2007).
13. Y. Jaluria and B. Gebhart, *J. Fluid Mech.*, **66**, 593 (1974).
14. O. Anwar Beg, Joaqun Zueco and H. S. Takhar, *Int. Commun. Heat Mass Transfer*, **35**, 810 (2008).
15. D. Y. Yoon, M. C. Kim and C. K.Choi, *Korean J. Chem. Eng.*, **20**, 27 (2003).
16. C.-Y. Cheng, *Int. Commum. Heat Mass Transfer*, **36**, 351 (2009).
17. A. C. Eringen, *J. Math. Mech.*, **16**, 1 (1966).
18. G. Lukaszewicz, *Micropolar fluids - Theory and applications*, Birkhauser, Basel (1999).
19. G. Ahmadi, *Int. J. Eng. Sci.*, **14**, 639 (1976).
20. D. A. S. Rees and I. Pop, *IMA J. Appl. Math.*, **61**, 179 (1998).
21. I. A. Hassanien, A. H. Essawy and N. M. Moursy, *Appl. Math. Comput.*, **152**, 323 (2004).
22. O. Abdulaziz and I. Hashim, *Numerical Heat Transfer, Part A: Applications*, **55**, 270 (2009).
23. J. Zueco, O. A. Beg and T. B. Chang, *Korean J. Chem. Eng.*, **26**, 1226 (2009).
24. F. Awad and P. Sibanda, *WSEAS Transactions on Heat and Mass Transfer*, **5**, 165 (2010).
25. M. M. Rahman, A. Aziz and M. A. Al-Lawatia, *Int. J. Therm. Sci.*, **49**, 993 (2010).
26. I. Anuar, *Meccanica*, **45**, 367 (2010).
27. N. Bachok, A. Ishak and R. Nazar, *HEAPFL'10 Proceedings of the 2010 International Conference on Theoretical and Applied Mechanics, and 2010 International Conference on Fluid Mechanics and Heat and Mass Transfer*, **26** (2010).
28. D. Srinivasacharya and Ch. RamReddy, *Int. Review Chem. Eng.*, **3**, 222 (2011).
29. T. Cebeci and P. Bradshaw, *Physical and computational aspects of convective heat transfer*, Springer-Verlag, New York (1984).
30. S. K. Jena and M. N. Mathur, *Int. J. Eng. Sci.*, **19**, 1431 (1991).
31. S. C. Cowin, *Phys. Fluids*, **11**, 1919 (1968).
32. S. L. Lee, T. S. Chen and B. F. Armaly, *ASME J. Heat Transfer*, **109**, 711 (1987).